PCCP

PAPER

View Article Online
View Journal | View Issue

Cite this: *Phys. Chem. Chem. Phys.*, 2015, **17**, 27035

Non-covalent intermolecular carbon–carbon interactions in polyynes†

Karunakaran Remya and Cherumuttathu H. Suresh*

Received 29th July 2015,
Accepted 14th September 2015

DOI: 10.1039/c5cp04467g

www.rsc.org/pccp

Polyynes, the smaller analogues of one dimensional infinite chain carbon allotrope carbyne, have been studied for the type and strength of the intermolecular interactions in their dimer and tetramer complexes using density functional theory. The nature of end group functionalities and the chain length of the polyynes are varied to assess their role in modulating the non-covalent interaction energy. As seen in molecular electrostatic potential analysis, all the polyyne complexes showed a multitude of non-covalent C···C interactions, resulting from complementary electrostatic interactions between relatively electron rich formal triple bond region of one monomer and the electron deficient formal single bond region of the other monomer. This type of paired (C≡C)···(C–C) bonding interaction, also characterized using quantum theory of atoms-in-molecules, increases with increase in the monomer chain length leading to substantial increase in interaction energy (E_{int}); −1.07 kcal mol^{-1} for the acetylene dimer to −45.83 kcal mol^{-1} for the 50yne dimer. The magnitude of E_{int} increases with substitutions at end positions of the polyyne and this effect persists even up to 50 triple bonds, the largest chain length analyzed in this paper. The role of C···C interactions in stabilizing the polyyne dimers is also shown by sliding one monomer in a dimer over the other, which resulted in multiple minima with a reduced number of C···C interactions and lower values of E_{int}. Furthermore, strong cooperativity in the C···C bond strength in tetramers is observed as the interaction energy per monomer (E_m) of the polyyne is 2.5–2.8 times higher compared to that of the dimer in a test set of four tetramers. The huge gain in energy observed in large polyyene dimers and tetramers predicts the formation of polyyne bundles which may find use in the design of new functional molecular materials.

Introduction

Carbyne ($(-C\equiv C-)_\infty$) is the sp hybridized allotrope of carbon consisting of single atom thin infinite chain of carbon atoms[1] while polyynes with the formula R(–C≡C)$_n$–R, the oligomeric analogues of carbyne are treated by chemists as a starting step towards the synthesis of carbynes. Polyynes are found to exist in meteorites,[2–3] biological sources,[4] carbon nanostructures[5] and mixed sp–sp^2 carbon structures.[6–7] Several polyynes containing metals and non-metals at their end positions have been characterized crystallographically.[8] Polyynes with several end groups have been synthesized and characterized.[9–13] Longer polyynes are found to be stable only with bulky substituents as their end groups.[14–15] Recently, polyynes containing up to 22 triple bonds that are stable under normal laboratory conditions have been synthesized and characterized by Chalifoux *et al.*[16] The end groups of the molecules synthesized by them include bulky groups containing Pt and Si which stabilized the polyyne backbone. The physical properties of carbyne are expected to be predicted by extrapolating the properties of polyynes.[10,16] The conjugated π electron circuit in polyyne can be tuned to obtain a low HOMO–LUMO gap suitable for the development of molecular conductors. Furthermore, the conjugation features of the π electrons in polyynes is not limited by rotation around single bonds,[17–18] which is the limitation of many other conducting organic compounds. Hence, polyynes are expected to form an important class of molecules forming one dimensional nanowires[19–27] in atomic scale circuits. They can also form spintronic devices[28] owing to their high mobility of electrons, hydrogen storage materials[29] and as structural components in atomic scale devices due to their favorable mechanical properties.[21,25,30–32]

However, to our knowledge, a detailed study on the nature of intermolecular interactions in polyynes is lacking in the literature. Similar to many other physical properties of polyynes that are affected by the nature of end groups,[21,33] the strength of intermolecular interactions in polyynes can also be susceptible to change with change in substitutions as well as the length of the molecule. Tuning the strengths of such interactions can

Chemical Sciences and Technology Division, CSIR-National Institute for Interdisciplinary Science and Technology, Trivandrum, 695 019, India. E-mail: sureshch@niist.res.in

† Electronic supplementary information (ESI) available. See DOI: 10.1039/c5cp04467g

help in the production of materials with desirable mechanical properties. Stronger intermolecular forces can lead to harder polyyne based materials. Studying the nature and strength of intermolecular interactions in polyynes with different substitutions can help predict their performance as structural and functional components. Intermolecular interactions involving carbon group elements have attracted increased attention in the area of non-covalent interactions.[34–45] A σ hole interaction[46–47] between an electron deficient carbon group element and an electron rich centre has been studied in detail[35] and is said to be comparable to other σ hole interactions such as halogen, chalcogen and pnicogen bonds.[48] The terms 'carbon bond'[34] and 'tetrel bonding'[36] have been introduced to denote such interactions of a σ hole on carbon and other carbon group elements respectively with electron rich donor sites.

In a previous study, we have shown that intermolecular interactions between similar carbon (C···C), nitrogen (N···N) and oxygen (O···O) atoms exists in several organic molecules.[49] The peculiarity of these interactions was that unlike usual intermolecular interactions between an electron rich donor and an electron deficient acceptor atom, the X···X (where X = C, N and O) interactions are formed between X atoms in similar chemical environments. These interactions were explained as resulting from the complimentary electrostatic interactions between electron rich and electron deficient regions on the interacting monomers. The Coulombic interactions in non-covalently interacting systems are described well by Politzer *et al.*[50] Natural bond order (NBO) analysis showed both the X atoms to be acting both as a donor and as an acceptor. Such interactions were shown to exist in the crystal structures of several organic molecules. In polyynes, alternating regions of electron density due to the presence of alternating triple bonds and formal single bonds can give rise to complementary Columbic interactions in polyyne dimers and higher order clusters.

In the present work, we analyze the types of intermolecular interactions in various polyyne molecules. The intermolecular C···C interactions studied in this paper do not fall under the classification of σ-hole interactions, which, by definition, are along the extension of a σ-bond. Instead, as shall be seen, the interactions are perpendicular to the polyyne molecules, between the chains. The effect of different end groups and chain lengths on the intermolecular C···C interactions in polyyne dimers is also studied. Dimers of polyyne molecules with H at one end and H, CN, NO_2, F, CF_3, and NMe_2 at the other end position are studied. Polyyne molecules with aforementioned substitutions and with 1, 2, 3, 4, 5, 10, 15, 20, 30, 40 and 50 triple bonds are selected for the study. A set of dimers with a donor group (NMe_2) at one end and an acceptor group (CN) at the other is also studied. Cooperativity of the C···C interactions is analyzed by studying a few tetramers.

Polyynes mentioned in this paper are named by their number of triple bonds and end groups other than hydrogen. For example, a polyyne molecule with five triple bonds and with a CN group at one end and H at the other is named as pentayne_CN. A polyyne molecule with four triple bonds and CN and NMe_2 as end groups is named as tetrayne_CN/NMe_2. Higher members are named by combining the number of triple bonds, the functional keyword –yne and the end group. For instance the name 50yne_CN indicates the polyyene with 50 triple bonds and the CN group at one end.

Computational methods

Polyynes containing one to five triple bonds are optimized using the M06L/6-311++g(d,p) level of theory.[51] For larger systems, a smaller basis set *viz.* 6-31g(d,p) is used with the same DFT method for optimization while single point energy calculations are done at the M06L/6-311++g(d,p) level. The geometries of polyynes containing up to 40 triple bonds have been confirmed to be minima by calculating the frequency. Frequency calculations of 50ynes have not been conducted due to high computational cost. However, since the trends in their geometries are similar to the lower analogues, we assume that the dimers of 50ynes are also minima. The calculations are done using Gaussian09[52] suit of programs. The excellent performance of the M06L functional with the 6-311++g(d,p) basis set compared to numerous other DFT methods available in Gaussian09 in calculating the geometry and interaction energy of weak non-covalent complexes has been previously shown by us in an extensive benchmark study.[53]

For further validation of the results, the dimers of monoynes and pentaynes with different end groups are studied using B97D[54] and the popular B3LYP[55–57] density functional along with the D2 version of Grimme's dispersion.[54] The interaction energies obtained using these methods are compared with the M06L values.

Considering that the molecular cluster is formed from the interaction of '*n*' monomer molecules, the total interaction energy (E_{int}) of the system can be calculated by using eqn (1).

$$E_{int} = E_{cluster} - (n)E_{monomer} + E_{bsse} \quad (1)$$

In eqn (1), $E_{cluster}$ is the energy of the cluster, $E_{monomer}$ is the energy of an isolated monomer and E_{bsse} is the counterpoise correction term by the Boys and Bernardy method[58] as implemented in Gaussian09. Cooperativity of the intermolecular interactions is studied by optimizing the tetramers and comparing the values of their interaction energy per monomer (E_m) with that of the dimers. The quantum theory of atoms-in-molecule (QTAIM)[59] as implemented in AIMAll[60] program is used to locate intermolecular interactions and compare their strength. QTAIM analysis gives (3, −1) critical points, referred to as bond critical points (BCPs) corresponding to bonding interactions. The value of electron density, ρ, at intermolecular BCPs is usually taken as a measure of the strength of such an interaction.[61–65] AIMAll generated images are used in the manuscript for describing the intermolecular interactions. Molecular electrostatic potential (MESP) is generally used as a tool for understanding intermolecular interactions.[66–68] Here, we have used MESP mapped at the 0.01 au isodensity surface

of the complexes to illustrate the Columbic nature of intermolecular interactions.

Results and discussion

Geometry and interaction energy of the dimers

Optimized geometry of the dimers of pentaynes with different end groups are given in Fig. 1. The dotted lines in the figure indicate intermolecular atom-to-atom interactions and their distances. In the next section, it will be revealed that all these interaction lines are characterized by the presence of a bond critical point (BCP) in the QTAIM analysis. Most of these interactions, except those towards the edges, are C···C interactions between carbon atoms in similar chemical environments. By this we mean that the interacting carbon atoms are chemically very similar.[49] From the C···C interaction lines shown in Fig. 1, it can be noticed that a formal CC triple bond towards the interior region of the dimer (the more localized bond in the distance range 1.21–1.24 Å shown in blue colour) shows two C···C interactions to a formal CC single bond (the more elongated CC bond in the distance range 1.32–1.34 Å). The bond length alternation behaviour of the polyynes is influenced by the nature of their end groups. The difference between adjacent single and triple bonds of pentaynes with different end groups are given in the ESI.† In the dimers of polyynes with H, F and CN as end groups, the only type of intermolecular interaction observed is the C···C interaction. In the dimers of polyynes substituted with CF_3, NO_2 and NMe_2, apart from C···C interactions, interactions between the end groups are also observed. However, the type of interaction that increases in number with increase in length of the monomers is the C···C interaction while the number of end group interactions remains the same in all the analogues in a series of polyynes. The C···C distances vary between 3.26–3.56 Å with most of them being around 3.40 Å, which is the typical range of values observed for the C···C interaction between carbon atoms in similar chemical environments.[49]

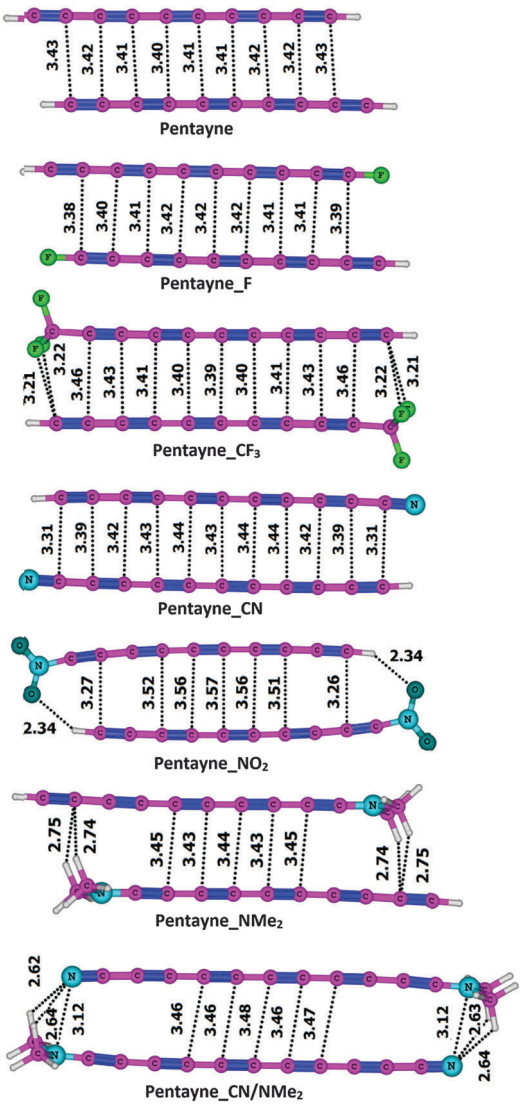

Fig. 1 Optimized geometries of pentayne dimers with different end groups. Formal triple bonded regions are shown in blue color. Distances are in Å.

In pentayne_CN and petayne_NO_2, the C···C distances are the shortest at the edges. An increase in the C···C distance towards the central part is clearly visible in these cases. Also in pentayne_F, though a clear variation is not visible, C···C distances are shortest at the edges. On the other hand, the intermolecular C···C distances in pentayne_CF_3 tend to decrease towards the central C···C interactions.

The counterpoise corrected interaction energies (E_{int}) of all the dimers containing up to 5 triple bonds and different end groups are given in Table 1. An increase in the value of E_{int} with increase in the number of triple bonds is clearly observed in all the cases. Since the interactions between the end groups in all the analogues are nearly the same, an increase in E_{int} with increase in length can be assigned solely due to the increased number of C···C interactions. Hence it is clear that the C···C interactions play a crucial role in the intermolecular interactions in longer polyyne derivatives. Among dimers with only C···C interactions as intermolecular interactions, pentayne_CN has the highest value for E_{int}. Dimers of oligoyynes with NMe_2 at one end and CN at the other end are significantly more stable compared to those with NMe_2 or CN at one end and H at the other.

The interaction energies of polyyne dimers with one and five triple bonds and different end groups obtained using B97D and B3LYPD2 density functionals are compared in Table 2. Comparing these values with the corresponding ones in Table 1,

Table 1 Counterpoise corrected interaction energy (E_{int}) of the dimers of oligoynes with different chain lengths and end groups (in kcal mol^{-1})

C≡C	H/H	H/F	H/CF_3	H/CN	H/NO_2	H/NMe_2	CN/NMe_2
1	−1.1	−1.1	−2.6	−3.2	−4.0	−4.8	−11.7
2	−1.0	−2.1	−3.4	−4.0	−4.8	−7.7	−12.7
3	−1.9	−3.1	−4.1	−4.9	−5.8	−8.5	−13.6
4	−2.7	−3.9	−5.2	−5.8	−6.8	−8.2	−14.5
5	−3.6	−4.8	−6.0	−6.7	−7.7	−8.9	−15.0

Table 2 Counterpoise corrected interaction energies (E_{int}, in kcal mol^{-1}) of acetylene and pentayne derivatives obtained using B97D and B3LYPD2 density functionals

	Acetylene derivatives		Pentayne derivatives	
End groups	B97D	B3LYPD2	B97D	B3LYPD2
H/H	−1.2	−1.4	−3.3	−3.3
H/F	−1.1	−1.4	−4.4	−4.9
H/CF_3	−2.4	−2.8	−5.7	−6.1
H/CN	−3.1	−3.3	−6.5	−6.7
H/NO_2	−4.0	−4.9	−7.8	−8.4
H/NMe_2	−4.5	−4.6	−10.7	−8.9
CN/NMe_2	−11.0	−11.9	−14.8	−15.0

it is clear that the trends in interaction energies given by these two methods are similar to those given by the M06L method. An increase in interaction energy with the chain length from 2 to 10 carbon atoms is shown by all the three DFT methods. The effect of end groups on the interaction energies is also found to be similar in all the three cases. That is, the lowest interaction energy is shown by dimers of unsubstituted polyynes (acetylene and pentayne) and the highest values are shown by polyynes with CN at one end and NMe_2 at the other end.

Analysis of Intermolecular bond critical points

The QTAIM analysis shows bond critical points (BCPs) corresponding to intermolecular C···C interactions in all the polyyne dimers studied. Fig. 2 depicts the QTAIM molecular graph of a few representative examples containing five triple bonds and the rest are given in the ESI.† The electron density (ρ) at

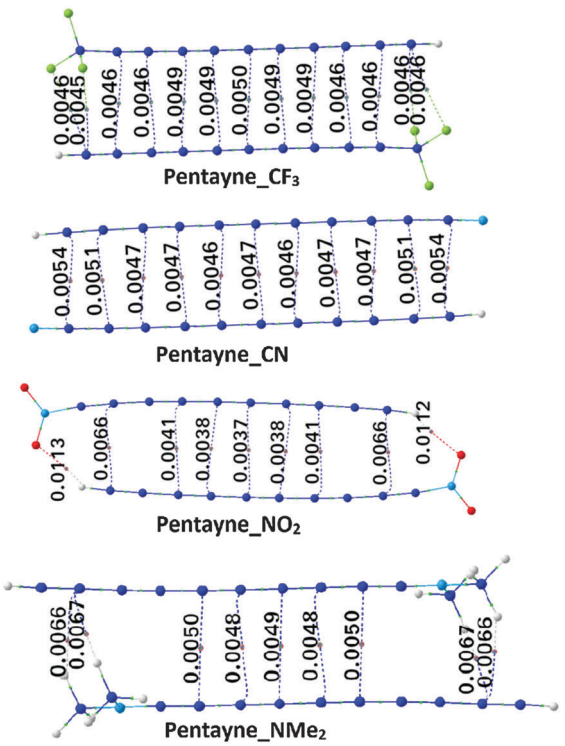

Fig. 2 QTAIM plot of pentayne dimers with different end groups. Values of electron density (ρ) at intermolecular BCPs are given in the figures in au.

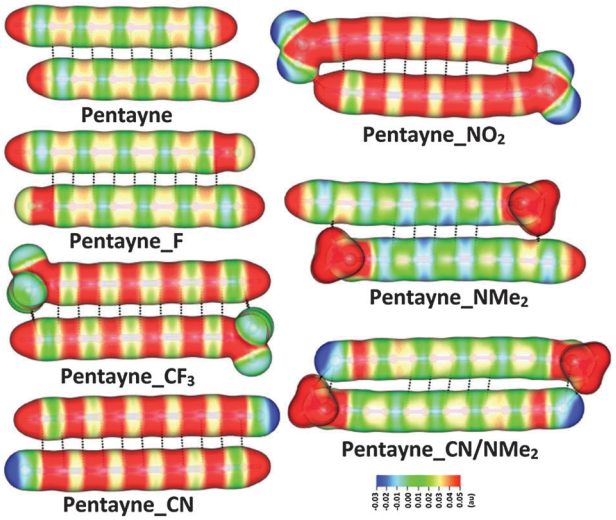

Fig. 3 Map of molecular electrostatic potential at 0.01 au isodensity surface of 5yne dimers with different end groups. Potential range: −0.03 to +0.05 au from blue to red.

intermolecular BCP is also depicted in the figures. The values of ρ (0.0037–0.0066 au) for these dimers are within the range of values observed for C···C interactions between similar carbon atoms[49] and other weak interactions such as 'carbon bonds'[34] and weak hydrogen bonds.[64] The trend in intermolecular bond strengths in each dimer is clear from the values of ρ at intermolecular BCPs. In pentayne_CN, pentayne_NO_2 and pentayne_F, the highest values of ρ towards the edges indicate strongest interactions. In dimers with CN and NO_2 end groups, the stronger end group interactions make the molecules a little bent inwards at the edges. Moreover, the presence of electron withdrawing end groups makes a higher difference in the electron density between the interacting carbon atoms towards the edges and the C···C interactions here become more of the 'donor–acceptor' type than an interaction between carbon atoms in similar chemical environments, and hence become stronger. This explains the curved geometry of these dimers where the shortest C···C interactions are observed towards the edge of the dimers. At the same time, in pentayne_CF_3, the highest ρ values are observed towards the interior, where the shortest C···C bonds are observed.

Explanation for C···C interactions based on molecular electrostatic potential

In our previous study, the formation of interactions between atoms in similar chemical environments is explained as resulting from complementary electrostatic interactions between electron rich and electron deficient regions of two interacting monomers.[49] In polyynes, the presence of alternate single and triple bonds can give rise to partitioning of the monomers into relatively electron rich and electron deficient regions. As a result complementary electrostatic interactions between electron rich regions on one monomer with electron deficient regions on another monomer arises. An illustration of the complementary electrostatic interactions in the dimers is given in Fig. 3 using the MESP maps of pentaynes (mapped at 0.01 au isodensity surface) with different

end groups. The similarity in the chemical nature of the interacting carbon atoms is clear from their similar MESP features. These maps show a partitioning of the constituent monomers into alternating rich, poor electron density regions throughout the length of the molecules to varying degrees in molecules with different end groups. From Fig. 3, it is clear that an end group can affect the distribution of electron density throughout the length of a molecule. It is also clear from the optimized geometry of the dimers given in Fig. 1 that the triple bond of one monomer is arranged close to the single bond of the second, resulting in a slightly shifted orientation of the oligoyne part of one monomer with respect to the other.

It is clear from the MESP figures that the entire complementary electrostatic regions in the dimers are contributing to the strength of the interaction. It may be noted that a bond path located in QTAIM analysis is useful to pin-point the major contributing atoms in the non-covalent bonding interaction whereas it cannot characterize the whole interacting region.[69] In pentayne_CN and pentayne_NO_2, a higher strength of C···C interactions towards the edges can be attributed to a larger difference in electrostatic potential between the interacting carbon atoms due to the presence of electron withdrawing groups.

Multiple minima with a lesser number of C···C interactions and lower interaction energy

The presence of a large number of alternating electron rich and electron deficient regions in polyynes suggests that any of the electron rich regions on a molecule can interact with any of the electron deficient regions on a second one. This also suggests the possibility of multiple minima on the potential energy surface of a dimer with a varying number of C···C interactions, while the global minimum could be the one showing the highest number of C···C interactions. Three dimers with only C···C interactions between their monomers *viz.* tetrayne, pentayne_F and tetrayne_CN are selected for illustrating this point. The QTAIM plots and MESP maps at the 0.01 au isosurface of the five minima located for the tetrayne_CN dimer are given in Fig. 4. The E_{int} values and the values of ρ at C···C BCPs of these minima are also marked in the figure. The QTAIM plots of the three minima located for the tetrayne dimer and the five minima located for the pentayne_F dimer along with their interaction energy and the value of ρ at C···C BCPs are given in the ESI.† These studies clearly show that several minima with difference in the number of C···C interactions can be located by sliding one of the monomers over the other. The interaction energy of the structures thus obtained decreases with decrease in the number of C···C interactions. Clearly, the one with the highest number of C···C interactions shows the highest stability, as indicated by the value of E_{int}. It is clear from Fig. 4 and Fig. S5 (ESI†) that the reduced number of C···C interactions results in a clear reduction in the value of E_{int} in all the three cases studied. This also proves that the C···C interactions play a key role in the stabilization of polyyne clusters. Alternating electron rich and electron deficient regions create

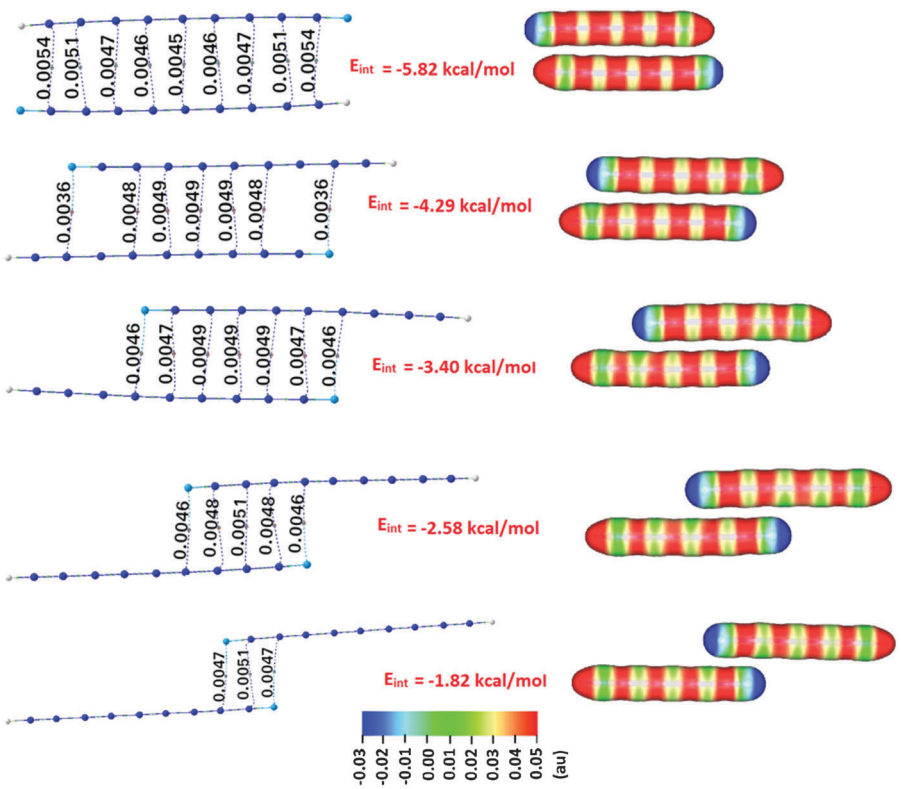

Fig. 4 QTAIM plot of five different minima located by sliding one of the monomers in the tetrayne_CN dimer over the other. The values of electron density (ρ) at intermolecular BCPs are given in au. Molecular electrostatic potential mapped at the 0.01 au isosurface of each minimum is also given. Potential range: −0.03 to +0.05 au from blue to red.

attractive Columbic interactions throughout the length of the polyyne molecules suggesting a multitude of stabilizing C···C interactions in the cluster.

Study of longer polyynes containing up to 100 carbon atoms

The possibility of extrapolating the intermolecular bonding behaviour to larger polyynes and finally to carbyne is tested by systematically increasing the number carbon atoms in the polyyne chain up to 100 carbon atoms (50 triple bonds). The value of E_{int} is found to increase with increase in the chain length in all the series of dimers having different end groups (Table 3). As the number of carbon atoms increases from 2 to 100 (acetylene dimer to 50yne dimer), the value of E_{int} increases from −1.07 kcal mol^{-1} to −45.83 kcal mol^{-1}. The effect of end groups on E_{int} values is also found to persist up to 100 carbon atoms. E_{int} values of dimers with substitutions other than hydrogen are higher than those with hydrogen at both ends. The series of polyyne dimers with the highest value for E_{int} is those with CN and NMe_2 as end groups.

The MESP maps of 50ynes with different end groups are given in Fig. 5. In all the cases, the geometry of the dimer is such that the electron rich region in one monomer is arranged near to the electron deficient region of the second resulting in complimentary electrostatic interactions. The effect of the end group on the value of E_{int} (and hence on the strength of C···C interactions) indicate that the end group's influence on the relative electron density on electron rich and electron deficient regions on the monomers can persists up to large chain lengths. This can be clearly visualized from the MESP maps given in Fig. 5 where a strong electron withdrawing end group causes a larger difference in electron density between the alternating regions of MESP on a polyyne molecule.

Table 3 Counterpoise corrected interaction energy (E_{int}) in kcal mol^{-1} of the dimers of polyynes with different chain lengths and end groups

C≡C	H/H	H/F	H/CF_3	H/CN	H/NO_2	H/NMe_2	CN/NMe_2
10	−8.3	−9.4	−10.4	−11.4	−12.4	−13.5	−20.2
15	−13.0	−14.0	−15.3	−16.1	−17.0	−18.2	−25.2
20	−17.7	−18.7	−20.0	−20.9	−21.8	−23.0	−30.1
30	−22.5	−27.7	−29.5	−30.3	−31.2	−32.4	−39.9
40	−37.2	−37.5	−38.6	−39.5	−40.6	−41.4	−49.2
50	−45.8	−45.7	−48.2	−49.0	−49.9	−51.1	−58.6

Effect of the dipole moment of polyyne molecules on the interaction energy

As seen in the previous section, the E_{int} values of the polyyne dimers increase with increase in the monomer chain length. The E_{int} values are also affected by the nature of end groups. A physical property that increases with increase in the length of the molecule and affected by the nature of the substituent is the dipole moment. The variation of the values of E_{int} with the dipole moment of interacting monomers (μ) is given in Fig. 6. It can be seen that the E_{int} values show a clear increase with increase in the value of μ. This is true in all the cases except for the unsubstituted polyynes (H at both the ends) where the monomer dipole moment is zero. This observation supports the assumption that the intermolecular C···C interactions are formed due to complimentary electrostatic interactions between the electron rich and electron deficient portions of the interacting monomers since an increase in the overall dipole moment can enhance the local dipoles throughout its length of a monomer and hence the strength of the C···C interactions. Thus, the series of polyyne analogues with highest values of μ shows the highest E_{int}. This can explain the highest

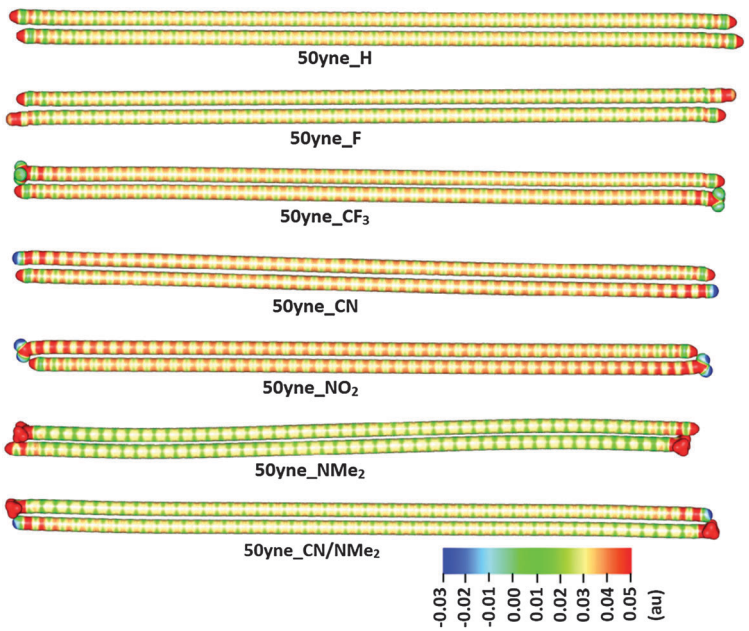

Fig. 5 Map of molecular electrostatic potential at 0.01 au isodensity surface of 50yne dimers with different end groups. Potential range: −0.03 to +0.05 au from blue to red.

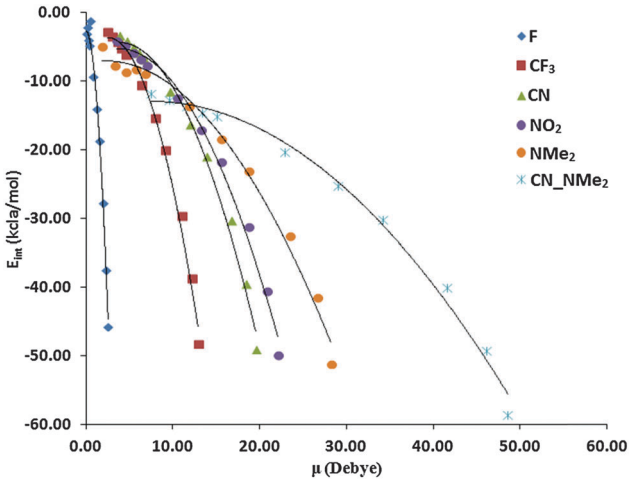

Fig. 6 Variation of E_{int} of the polyyne dimers with monomer dipole moment (μ).

values of E_{int} in dimers of oligoyynes substituted with CN at one end and NMe_2 at the other.

Tetramers

The presence of a large number of electron rich and electron poor regions throughout the length of polyyne as well as their cylindrical symmetry implies that more than one molecule can be self-assembled around one monomer leading to molecular clusters provided that the stabilizing C···C interactions retain their strength in a larger cluster. In order to test this hypothesis, tetramers of pentayne, pentayne_F, 10yne and 10yne_F are selected for the study of formation of higher order tetramer clusters. Optimized geometries of these structures are given in Fig. 7.

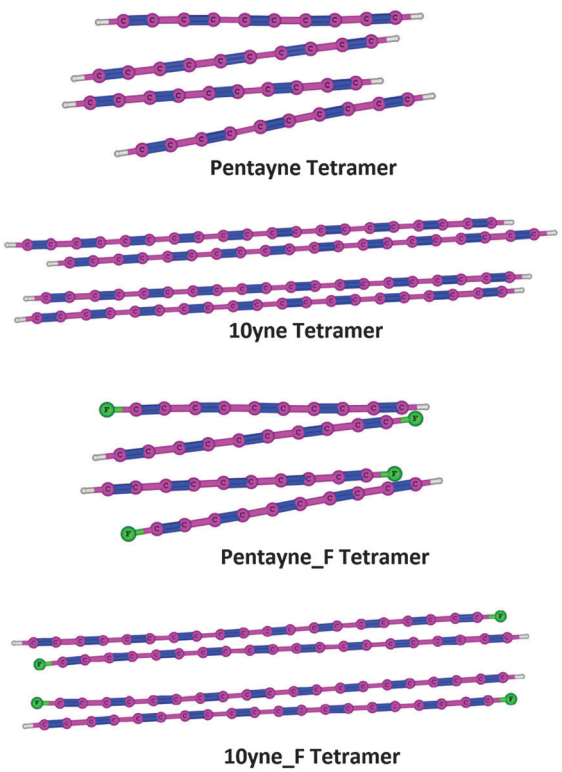

Fig. 7 Optimized geometry of the tetramers.

Table 4 E_{int} and E_m values of the tetramers and E_m values of the corresponding dimers

Tetramer of	E_{int} (kcal mol^{-1})	E_m (kcal mol^{-1})	E_m of dimer (kcal mol^{-1})
5yne	−20.0	−5.0	−1.8
5yne_F	−24.4	−6.1	−2.4
10yne	−47.0	−11.8	−4.2
10yne_F	−52.1	−13.0	−4.7

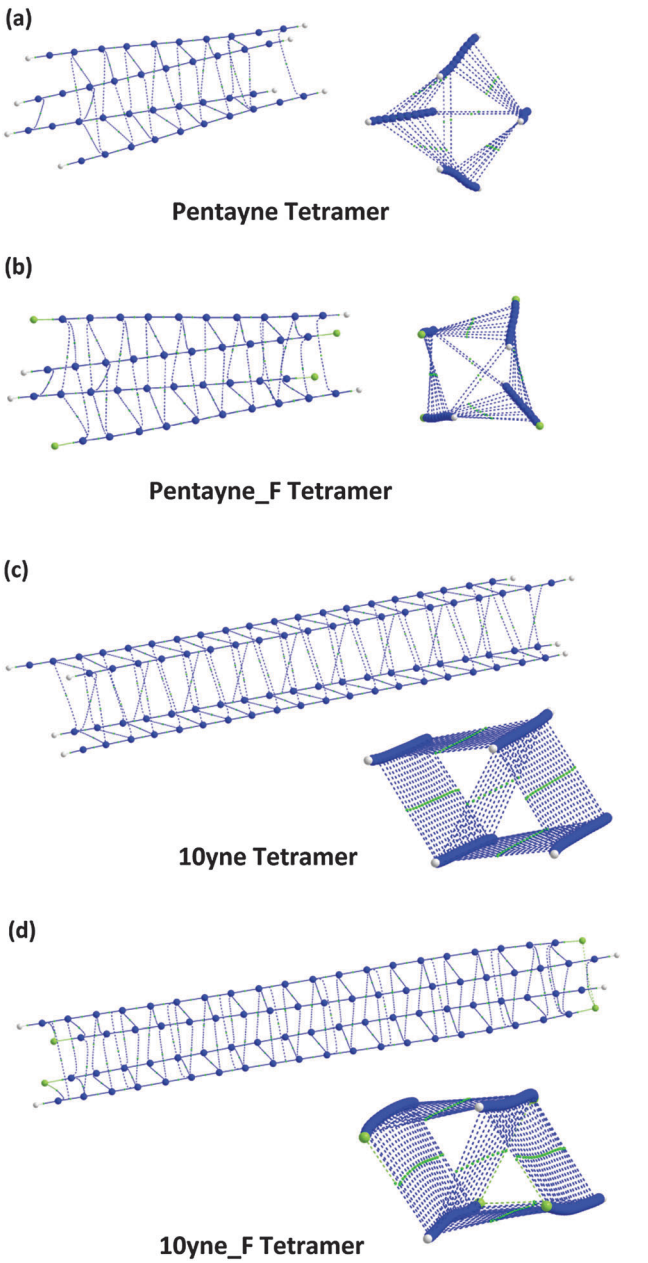

Fig. 8 Two different orientations of the QTAIM plot of (a) Pentayne tetramer, (b) Pentayne _F tetramer, (c) 10yne tetramer and (d) 10yne_F tetramer.

The E_{int} and interaction energy per monomer (E_m) values of the tetramers and E_m values of the corresponding dimers are given in Table 4. Interaction energy of all these tetramers showed a drastic increase (more than 5 times in all the cases) compared to the dimers. For instance, the value of E_{int} of 3.6 kcal mol^{-1} for the pentayne dimer increases to 20.0 kcal mol^{-1} for its tetramer. These results clearly suggest that in higher order clusters, large cooperativity in C···C interactions exists which may drive the system to form self-assembled molecular wire like materials.

The QTAIM plots of the tetramers are given in Fig. 8. The large increase in E_{int} values on going from dimer to tetramer can be attributed to the increase in the number of C···C interactions. Since each of the monomer can interact with two other monomers in the tetramers, one would expect four sets of C···C interactions. However, including the interactions between the monomers in diagonal positions, five sets of interactions are observed in the QTAIM analysis. The most gratifying is the fact that even in the context of multiple C···C interactions from the same carbon atoms, the strength of individual C···C interactions is not deteriorated due to large cooperativity in intermolecular interactions.

Conclusions

Non-covalent interactions in seven series of polyyne dimers wherein the constituent monomers possess 1, 2, 3, 4, 5, 10, 15, 20, 30, 40 and 50 CC triple bonds and different substitutions at their end positions have been studied using density functional theory. The C···C interactions between carbon atoms in similar chemical environments are the most important type of intermolecular interaction in these molecular complexes. The number of C···C interactions increases with the increase in the monomer chain length leading to substantial stabilization of the dimers. For each series of dimers, since the number of interaction between the end groups remain the same for all chain lengths, the increase in interaction energy is fully accounted by the increase in the number of C···C interactions. Such interactions result from complimentary electrostatic interactions between relatively electron rich formal triple bond regions and electron deficient formal single bond regions in the interacting monomers. The MESP map is useful to visualize the complementary electrostatic interaction in the dimers. The nature of the end group has a strong influence on the strength of C···C interactions and it persists even up to a 100 carbon atom chain length, which is the largest system studied in this paper. This suggests that tuning the intermolecular interaction energies can be made possible by selecting appropriate end groups. The E_{int} values are also influenced by the dipole moment of the end group substituted monomers which increases with increase in the chain length. A dimer can have several minima with different number of C···C interactions on its potential energy surface, the one having the highest number of C···C interactions is always located as the global minimum. This observation clearly demonstrates the role of C···C interactions in stabilizing the supramolecular complexes of polyynes. Due to the cylindrical nature of the electron distribution in polyynes, higher order clusters showing multiple complementary electrostatic interactions from the same CC region in different lateral directions is possible leading to further enhancement in the stability of the cluster. This effect is huge and the tetramers showed more than five-fold increase in the total interaction energy compared to the dimers and this brings out the strong cooperativity in cluster formation of the polyyne molecules. These results clearly suggest that long chain polyynes are promising materials for the development of molecular wire-like materials for structural and functional applications.

Acknowledgements

This research work is supported by the Council of Scientific and Industrial Research (CSIR), Govt. of India, through a project CSC0129. K.R. is thankful to CSIR, India, for providing a senior research fellowship.

References

1 R. B. Heimann, J. Kleiman and N. M. Salansky, *Nature*, 1983, **306**, 164–167.
2 R. Hayatsu, R. G. Scott, M. H. Studier, R. S. Lewis and E. Anders, *Science*, 1980, **209**, 1515–1518.
3 A. G. Whittaker, E. J. Watts, R. S. Lewis and E. Anders, *Science*, 1980, **209**, 1512–1514.
4 A. L. K. Shi Shun and R. R. Tykwinski, *Angew. Chem., Int. Ed.*, 2006, **45**, 1034–1057.
5 L. Ravagnan, F. Siviero, C. Lenardi, P. Piseri, E. Barborini, P. Milani, C. S. Casari, A. Li Bassi and C. E. Bottani, *Phys. Rev. Lett.*, 2002, **89**, 285506.
6 C. S. Casari, A. Li Bassi, A. Baserga, L. Ravagnan, P. Piseri, C. Lenardi, M. Tommasini, A. Milani, D. Fazzi, C. E. Bottani and P. Milani, *Phys. Rev. B: Condens. Matter Mater. Phys.*, 2008, **77**, 195444.
7 L. Ravagnan, P. Piseri, M. Bruzzi, S. Miglio, G. Bongiorno, A. Baserga, C. S. Casari, A. Li Bassi, C. Lenardi, Y. Yamaguchi, T. Wakabayashi, C. E. Bottani and P. Milani, *Phys. Rev. Lett.*, 2007, **98**, 216103.
8 S. Szafert and J. A. Gladysz, *Chem. Rev.*, 2003, **103**, 4175–4206.
9 F. Cataldo, L. Ravagnan, E. Cinquanta, I. E. Castelli, N. Manini, G. Onida and P. Milani, *J. Phys. Chem. B*, 2010, **114**, 14834–14841.
10 W. A. Chalifoux and R. R. Tykwinski, *C. R. Chim.*, 2009, **12**, 341–358.
11 S. Eisler, A. D. Slepkov, E. Elliott, T. Luu, R. McDonald, F. A. Hegmann and R. R. Tykwinski, *J. Am. Chem. Soc.*, 2005, **127**, 2666–2676.
12 A. D. Slepkov, F. A. Hegmann, S. Eisler, E. Elliott and R. R. Tykwinski, *J. Chem. Phys.*, 2004, **120**, 6807–6810.
13 C. Wang, A. S. Batsanov, K. West and M. R. Bryce, *Org. Lett.*, 2008, **10**, 3069–3072.

14 T. Gibtner, F. Hampel, J.-P. Gisselbrecht and A. Hirsch, *Chem. – Eur. J.*, 2002, **8**, 408–432.
15 Q. Zheng, J. C. Bohling, T. B. Peters, A. C. Frisch, F. Hampel and J. A. Gladysz, *Chem. – Eur. J.*, 2006, **12**, 6486–6505.
16 W. A. Chalifoux and R. R. Tykwinski, *Nat. Chem.*, 2010, **2**, 967–971.
17 J. Chen and M. A. Reed, *Chem. Phys.*, 2002, **281**, 127–145.
18 J. Taylor, M. Brandbyge and K. Stokbro, *Phys. Rev. B: Condens. Matter Mater. Phys.*, 2003, **68**, 121101.
19 Ž. Crljen and G. Baranović, *Phys. Rev. Lett.*, 2007, **98**, 116801.
20 N. D. Lang and P. Avouris, *Phys. Rev. Lett.*, 2000, **84**, 358–361.
21 M. Liu, V. I. Artyukhov, H. Lee, F. Xu and B. I. Yakobson, *ACS Nano*, 2013, **7**, 10075–10082.
22 N. D. Lang and P. Avouris, *Phys. Rev. Lett.*, 1998, **81**, 3515–3518.
23 S. Ballmann, W. Hieringer, D. Secker, Q. Zheng, J. A. Gladysz, A. Görling and H. B. Weber, *ChemPhysChem*, 2010, **11**, 2256–2260.
24 F. Börrnert, C. Börrnert, S. Gorantla, X. Liu, A. Bachmatiuk, J.-O. Joswig, F. R. Wagner, F. Schäffel, J. H. Warner, R. Schönfelder, B. Rellinghaus, T. Gemming, J. Thomas, M. Knupfer, B. Büchner and M. H. Rümmeli, *Phys. Rev. B: Condens. Matter Mater. Phys.*, 2010, **81**, 085439.
25 A. K. Nair, S. W. Cranford and M. J. Buehler, *Europhys. Lett.*, 2011, **95**, 16002.
26 K. H. Khoo, J. B. Neaton, Y. W. Son, M. L. Cohen and S. G. Louie, *Nano Lett.*, 2008, **8**, 2900–2905.
27 C. Wang, A. S. Batsanov, M. R. Bryce, S. Martín, R. J. Nichols, S. J. Higgins, V. M. García-Suárez and C. J. Lambert, *J. Am. Chem. Soc.*, 2009, **131**, 15647–15654.
28 Z. Zanolli, G. Onida and J. C. Charlier, *ACS Nano*, 2010, **4**, 5174–5180.
29 P. B. Sorokin, H. Lee, L. Y. Antipina, A. K. Singh and B. I. Yakobson, *Nano Lett.*, 2011, **11**, 2660–2665.
30 J. K. Ashley, Y. Neta Aditya Reddy and W. C. Steven, *Nanotechnology*, 2014, **25**, 335709.
31 A. J. Kocsis, N. A. R. Yedama and S. W. Cranford, *Nanotechnology*, 2014, **25**, 335709.
32 R. Mirzaeifar, Z. Qin and M. J. Buehler, *Nanotechnology*, 2014, **25**, 371001.
33 L. Ravagnan, N. Manini, E. Cinquanta, G. Onida, D. Sangalli, C. Motta, M. Devetta, A. Bordoni, P. Piseri and P. Milani, *Phys. Rev. Lett.*, 2009, **102**, 245502.
34 D. Mani and E. Arunan, *Phys. Chem. Chem. Phys.*, 2013, **15**, 14377–14383.
35 A. Bundhun, P. Ramasami, J. Murray and P. Politzer, *J. Mol. Model.*, 2013, **19**, 2739–2746.
36 A. Bauzá, T. J. Mooibroek and A. Frontera, *Angew. Chem., Int. Ed.*, 2013, **52**, 12317–12321.
37 L. M. Azofra, M. M. Quesada-Moreno, I. Alkorta, J. R. Aviles-Moreno, J. J. Lopez-Gonzalez and J. Elguero, *New J. Chem.*, 2014, **38**, 529–538.
38 A. Bauzá, R. Ramis and A. Frontera, *Comput. Theor. Chem.*, 2014, **1038**, 67–70.
39 S. J. Grabowski, *Phys. Chem. Chem. Phys.*, 2014, **16**, 1824–1834.
40 Q. Li, X. Guo, X. Yang, W. Li, J. Cheng and H.-B. Li, *Phys. Chem. Chem. Phys.*, 2014, **16**, 11617–11625.
41 S. A. C. McDowell, *Chem. Phys. Lett.*, 2014, **598**, 1–4.
42 S. A. C. McDowell and J. A. Joseph, *Phys. Chem. Chem. Phys.*, 2014, **16**, 10854–10860.
43 S. P. Thomas, M. S. Pavan and T. N. Guru Row, *Chem. Commun.*, 2014, **50**, 49–51.
44 P. R. Varadwaj, A. Varadwaj and B.-Y. Jin, *Phys. Chem. Chem. Phys.*, 2014, **16**, 17238–17252.
45 D. Mani and E. Arunan, *J. Phys. Chem. A*, 2014, **118**, 10081–10089.
46 T. Clark, M. Hennemann, J. Murray and P. Politzer, *J. Mol. Model.*, 2007, **13**, 291–296.
47 J. Murray, P. Lane and P. Politzer, *J. Mol. Model.*, 2009, **15**, 723–729.
48 P. Politzer, J. S. Murray and T. Clark, *Phys. Chem. Chem. Phys.*, 2013, **15**, 11178–11189.
49 K. Remya and C. H. Suresh, *Phys. Chem. Chem. Phys.*, 2015, **17**, 18380–18392.
50 P. Politzer, J. Murray and T. Clark, *J. Mol. Model.*, 2015, **21**, 1–10.
51 Y. Zhao and D. G. Truhlar, *J. Chem. Phys.*, 2006, **125**, 194101.
52 M. J. Frisch, G. W. Trucks, H. B. Schlegel, G. E. Scuseria, M. A. Robb, J. R. Cheeseman, G. Scalmani, V. Barone, B. Mennucci, G. A. Petersson, H. Nakatsuji, M. Caricato, X. Li, H. P. Hratchian, A. F. Izmaylov, J. Bloino, G. Zheng, J. L. Sonnenberg, M. Hada, M. Ehara, K. Toyota, R. Fukuda, J. Hasegawa, M. Ishida, T. Nakajima, Y. Honda, O. Kitao, H. Nakai, T. Vreven, J. J. A. Montgomery, J. E. Peralta, F. Ogliaro, M. Bearpark, J. J. Heyd, E. Brothers, K. N. Kudin, V. N. Staroverov, T. Keith, R. Kobayashi, J. Normand, K. Raghavachari, A. Rendell, J. C. Burant, S. S. Iyengar, J. Tomasi, M. Cossi, N. Rega, J. M. Millam, M. Klene, J. E. Knox, J. B. Cross, V. Bakken, C. Adamo, J. Jaramillo, R. Gomperts, R. E. Stratmann, O. Yazyev, A. J. Austin, R. Cammi, C. Pomelli, J. W. Ochterski, R. L. Martin, K. Morokuma, V. G. Zakrzewski, G. A. Voth, P. Salvador, J. J. Dannenberg, S. Dapprich, A. D. Daniels, O. Farkas, J. B. Foresman, J. V. Ortiz, J. Cioslowski and D. J. Fox, *Gaussian 09, Revision D.01*, Gaussian, Inc., Wallingford CT, 2010.
53 K. Remya and C. H. Suresh, *J. Comput. Chem.*, 2013, **34**, 1341–1353.
54 S. Grimme, *J. Comput. Chem.*, 2006, **27**, 1787–1799.
55 A. D. Becke, *J. Chem. Phys.*, 1993, **98**, 5648–5652.
56 C. Lee, W. Yang and R. G. Parr, *Phys. Rev. B: Condens. Matter Mater. Phys.*, 1988, **37**, 785–789.
57 B. Miehlich, A. Savin, H. Stoll and H. Preuss, *Chem. Phys. Lett.*, 1989, **157**, 200–206.
58 S. F. Boys and F. Bernardi, *Mol. Phys.*, 1970, **19**, 553–566.
59 R. F. W. Bader, *Atoms in Molecules: A Quantum Theory*, Clarendon Press, Oxford, 1990.
60 T. A. Keith, *AIMAll (Version 14.04.17)*, TK Gristmill Software, Overland Park KS, USA, 2014.

61 O. Knop, K. N. Rankin and R. J. Boyd, *J. Phys. Chem. A*, 2002, **107**, 272–284.
62 S. J. Grabowski, *J. Phys. Chem. A*, 2001, **105**, 10739–10746.
63 K. Remya and C. H. Suresh, *J. Comput. Chem.*, 2014, **35**, 910–922.
64 R. Parthasarathi, V. Subramanian and N. Sathyamurthy, *J. Phys. Chem. A*, 2006, **110**, 3349–3351.
65 P. L. A. Popelier, *J. Phys. Chem. A*, 1998, **102**, 1873–1878.
66 P. Politzer and D. G. Truhlar, *Chemical Applications of Atomic and Molecular Electrostatic Potentials: Reactivity, Structure, Scattering: Energetics of Organic, Inorganic, and Biological Systems*, Springer, New York, 1981.
67 J. S. Murray and K. Sen, *Molecular Electrostatic Potentials: Concepts and Applications*, Elsevier Science, Amsterdam, The Netherlands, 1996.
68 S. R. Gadre and R. N. Shirsat, *Elelectrostatics of Atoms and Molecules*, Universities Press, Hyderabad, India, 2000.
69 C. Foroutan-Nejad, S. Shahbazian and R. Marek, *Chem. – Eur. J.*, 2014, **20**, 10140–10152.

